Neuro-Oncology Advances
7(1), vdae233, 2025 | https://doi.org/10.1093/noajnl/vdae233 | Advance Access date 23 December 2024

Cuproplasia-related gene signature: Prognostic insights for glioma therapy

Toni Rose Jue, Joseph Descallar, Vu Viet Hoang Pham, Jessica Lilian Bell, Tyler Shai-Hee, Riccardo Cazzolli, Sumanth Nagabushan, Eng-Siew Koh, and Orazio Vittorio

All author affiliations are listed at the end of the article

Corresponding Author: Associate Professor Orazio Vittorio, School of Biomedical Sciences, Faculty of Medicine and Health – Lowy Cancer Research Centre, Cnr Botany & High Street, UNSW Kensington Campus, Sydney, NSW, Australia 1466 (Orazio.vittorio@unsw.edu.au).

Abstract

Background. Adult-type diffuse gliomas encompass nearly a quarter of all primary tumors found in the CNS, including astrocytoma, oligodendroglioma, and glioblastoma. Histopathological tumor grade and molecular profile distinctly impact patient survival. Despite treatment advancements, patients with recurrent glioma have a very poor clinical outcome, warranting improved risk stratification to determine therapeutic interventions. Various studies have shown that copper is a notable trace element that is crucial for biological processes and has been shown to display pro-tumorigenic functions in cancer, particularly gliomas.

Methods. Differential gene expression, Cox regression, and least absolute shrinkage and selection operator regression were used to identify 19 copper-homeostasis-related gene signatures using TCGA lower-grade glioma and glioblastoma (GBM) cohorts. The GLASS Consortium dataset was used as an independent validation cohort. Enrichment analysis revealed the involvement of the signature in various cancer-related pathways and biological processes. Using this CHRG signature, a risk score model and a nomogram were developed to predict survival in glioma patients.

Results. Our prognostic CHRG signature stratified patients into high- and low-risk groups, demonstrating robust predictive performance. High-risk groups showed poorer survival outcomes. The nomogram model integrating CHRG signature and clinical features accurately predicted 1-, 3-, and 5-year survival rates in both training and test sets.

Conclusions. The identified 19-gene CHRG signature holds promise as a prognostic tool, enabling accurate risk stratification and survival prediction in glioma patients. Integrating this signature with clinical characteristics enhances prognostic accuracy, underscoring its potential clinical utility in optimizing therapeutic strategies and patient care in glioma management.

Key Points

- 19-CHRG signature accurately predicts survival in glioma patients.
- High-risk patients have significantly worse survival than the low-risk group.
- Risk model can guide patient stratification for copper-targeted treatment.

Adult-type diffuse gliomas comprise approximately 24% of all primary CNS tumors and encompass several pathologies including isocitrate dehydrogenase (IDH)-mutant astrocytoma, IDH-mutant and 1p/19q co-deleted oligodendrogliomas and IDH-wild type GBM.[1,2] Almost 80% of patients with a malignant brain tumor are diagnosed with either of these subtypes. Histopathological grade and the molecular profiles of the tumors influence median survival, ranging from 14 months in

Importance of the Study

Copper-targeting drugs have undergone clinical trials as anti-cancer agents and have shown positive outcomes in various cancer types such as breast cancer, lung cancer, and melanoma. On the contrary, copper-targeting therapies examined in clinical trials with patients diagnosed with gliomas have not resulted in a positive outcome. We believe this can be attributed to the lack of patient stratification to determine which patients are molecularly compatible with copper-targeting treatment. This study identified a 19-CHRG signature that can be used to determine the survival risk of patients and possibly stratify patients who can receive copper-targeting drugs. With recent developments in the link of copper in immune modulation, we believe this 19-CHRG signature can also be used to stratify patients into appropriate immune-targeted therapies.

GBM patients to 199 months in patients with oligodendroglial tumors.[2] Treatment decisions are based on tumor subtype which may include maximal surgical resection with chemoradiotherapy or a watch-and-wait approach. Survival benefits have not changed despite the standard of care treatment, with most tumors inevitably undergoing recurrence with a worse prognosis. A better understanding of the risk categories is needed to improve therapeutic approaches, patient survival, and patient quality of life.

Copper is an essential trace element that plays a critical role in various biological processes, through its utilization as a cofactor for several enzymes (cuproenzymes). Examples include cytochrome c oxidase, superoxide dismutase, and ceruloplasmin which aid in the facilitation of ATP (Adenosine triphosphate) synthesis, prevention of reactive oxygen species formation, and iron metabolism respectively. Copper homeostasis is strictly regulated in the human body, as excessive copper accumulation is toxic and can result in the generation of reactive oxygen species. Abnormalities in genes responsible for regulating copper homeostasis result in the recessive disorders Menkes and Wilson's Disease, characterized by copper deficiency and excessive copper accumulation respectively. Elevated serum and tissue copper levels have been reported in various cancer types including malignant gliomas.[3,4] Copper has been associated with a broad spectrum of pro-tumorigenic functions including angiogenesis, metastasis, and immune evasion,[5–7] indicating the reliance of malignant cells on copper for survival. Moreover, recent literature has shown how intracellular copper levels can modulate immune checkpoint expression such as Programmed Death-Ligand 1 (PD-L1).[6] Thus, understanding whether a copper-homeostasis-related gene signature can be used as a predictor of survival and as a tool to personalize copper-targeting therapeutic approaches for glioma is needed.

Recently, copper-related gene signatures have been widely studied in various cancer types including gliomas.[8–22] With our knowledge that copper is involved in multifaceted levels of tumorigenesis and normal cell biology, the low number of genes analyzed put a limitation on existing copper gene signatures. It is needed to expand this gene set to gain a deeper understanding of the prognostic value of copper-homeostasis-related genes (CHRGs).

In this study, we analyzed the expression of 133 CHRGs using TCGA GBM and lower-grade glioma (LGG) datasets. Of these 19 prognostic CHRGs were used to stratify patients into high- and low-risk relative to overall survival. The ability to tailor interventions based on a patient's molecular profile holds promise for improving treatment outcomes. Classification of risk groups along with other clinical features typically observed in patients with glioma can be used as a prognostic marker and could be used to stratify patients for future clinical trials to test copper-targeting therapies in combination with immunotherapies.

Materials and Methods

Assembly of Copper Homeostasis Related Gene Set

Gene sets annotated with the keyword "copper" were obtained from Molecular Signatures Database (MSigDB v7.5.1) including WP_COPPER_HOMEOSTASIS, HP_DECREASED_CIRCULATING_COPPER_CONCENTRATION, HP_ABNORMAL_CIRCULATING_COPPER_CONCENTRATION, GOMF_COPPER_ION_TRANSMEMBRANE_TRANSPORTER_ACTIVITY, GOMF_COPPER_ION_BINDING, GOMF_COPPER_CHAPERONE_ACTIVITY,GOBP_RESPONSE_TO_COPPER_ION, GOBP_DETOXIFICATION_OF_COPPER_ION, GOBP_COPPER_ION_TRANSPORT, GOBP_COPPER_ION_TRANSMEMBRANE_TRANSPORT, GOBP_COPPER_ION_IMPORT, GOBP_COPPER_ION_HOMEOSTASIS, GOBP_CELLULAR_RESPONSE_TO_COPPER_ION, GOBP_CELLULAR_COPPER_ION_HOMEOSTASIS. The union of all gene sets resulted in 133 genes being included in the final CHRG set for analysis.

Datasets

Messenger ribonucleic acid (mRNA) expression and survival data from the GDC (Genomic Data Commons) TCGA GBM ($n = 173$), GDC TCGA LGG ($n = 529$), and GTEx (Genotype-Tissue Expression) normal brain cortex samples ($n = 105$) were downloaded from UCSC Xena.[23] Clinical annotations were downloaded from the TCGAbiolinks package in R. mRNA expression and clinical annotations from the Glioma Longitudinal Analysis (GLASS) Consortium were downloaded from Synapse (https://www.synapse.org/glass).[24]

Both TCGA and GLASS datasets comply with the 2000 and 2007 CNS World Health Organization (WHO) classification primarily based on histopathological features.[25] These datasets were re-annotated so that samples comply with the WHO CNS5 nomenclature (Supplementary Figure

1). Re-annotation was performed based on molecular markers, including IDH mutation status, 1p/19q codeletion status, EGFR amplification, and TERT promoter mutation status. Grading was reassessed using CDKN2A/B homozygous deletion information.

TCGA GBM and LGG datasets were combined and randomly partitioned into a 70% training and a 30% test set using the Base R method. The GLASS dataset was used as an independent cohort for validation. Only patients over 18 years old and with survival data were included in the analysis.

Identification of Differential Expressed CHRGs

Differentially expressed genes (DEG) between normal cortex samples and TCGA glioma samples (training set) were analyzed using the "DESeq2," "EdgeR" and "limma-voom" packages for R version 4.2.2 (2022-10-31). Further feature selection was performed using a threshold cutoff of log2 |fold change| > 1 and adjusted $P < .05$. Venn diagram analysis was used to determine the intersection between the 3 algorithms used for DEG analysis.

Risk Score Construction and Validation

To determine the prognostic value of the differentially expressed CHRGs, univariate Cox proportional hazards regression model analysis was performed on the training set using "ezcox" (ie, https://github.com/ShixiangWang/ezcox) package in R. Genes showing statistically significant ($P < .05$) effect on patient survival were selected for further analyses.

To minimize the risk of over-fitting, least absolute shrinkage and selection operator (LASSO)-Cox regression was used to construct a risk score model from "glmnet" package.[26] We used glmnet with $\alpha = 1$ (ie, LASSO penalty) and ten-fold cross-validation to tune the L1 regularization parameter λ. Two different datasets were used, the "training" dataset ($n = 465$) was used to train the risk score model, while the "test" dataset ($n = 205$) and GLASS dataset ($n = 153$) were used for validation. The LASSO Cox regression model was fitted using the training dataset to identify CHRGs which had effects on survival, and the identified CHRGs were considered as a risk signature.

The risk score model was established as:

$$S = \sum_{i=1}^{n} e_i \times c_i,$$

where S is the risk score, n is the number of genes in the risk signature, e_i is the expression of gene i, c_i is the coefficient of gene i. Risk scores were calculated for each patient in both the training and test datasets using the normalized expression level of each CHRG and corresponding regression coefficients produced from the training dataset (see formula above). These were then evaluated based on survival data. The receiver operating characteristic (ROC) curve was plotted, and the AUC was computed using the R package of "timeROC."[27]

Patients were subsequently stratified into low- and high-risk groups based on a median score determined from the training dataset.

Nomogram Development and Evaluation

We developed a nomogram to offer clinicians a quantitative tool for predicting the prognoses of patients diagnosed with GBM, astrocytoma, oligodendroglioma, or oligoastrocytoma. This nomogram relies on factors such as age, gender, and the risk group based on the expression of the prognostic CHRG signature. Its purpose is to predict the survival rates at 1, 3, and 5 years for these patients.

Initially, we conducted a Univariate Cox analysis to identify clinicopathological variables that individually contributed as prognostic predictors for patient overall survival (OS). Subsequently, those variables demonstrating significance ($P < .05$) in their predictive capacity were incorporated into a multivariable Cox regression analysis. Finally, utilizing the outcomes of the multivariable Cox regression analysis, we created a nomogram using the "rms" package. The accuracy of the model was assessed by analyzing the concordance index (C-Index), calibration curves, and ROC analysis to ascertain its prognostic value.

Immunohistochemistry (IHC) Validation of Prognostic CHRGs

IHC images were retrieved from the Human Protein Atlas online database (http://www.proteinatlas.org).[28] Details and URL access to the images of prognostic CHRG with available data are shown in Supplementary Table 1.

Gene Set Enrichment Analysis

Gene set enrichment analysis was performed using Enrichr on the 19 prognostic CHRG signature.[29] Enrichr was used to identify gene set enrichments in Gene Ontology (GO) Biological Processes and GO Molecular Function, as well as pathway enrichment from the Reactome database.

Dependency Score Analysis

The median mRNA abundance (RNA-sequencing—Expression Public 23Q4) and median dependency scores (24Q2, Chronos) from the DepMap website (https://depmap.org/portal/), data was provided by the Broad Institute Cancer Dependency Map Expression Public 24Q2 were analyzed. The lower the dependency score, the more essential the gene is for cell survival and/or proliferation. Positive scores indicate increased growth rate/cell survival compared to the parental cells when the gene is genetically deleted, whereas negative scores reflect gene knockout has a negative impact on cell growth (https://doi.org/10.25452/figshare.plus.25880521.v1).[30]

Inference of Immune Cell Proportions

The overall abundance of 22 immune cell types was measured using the CIBERSORT deconvolution algorithm.[31,32] Briefly, mRNA expression of TCGA GBM and LGG cohorts were uploaded to the CIBERSORT website (http://cibersort.stanford.edu/). Absolute immune fraction scores for each

patient sample were estimated based on the "LM22" gene signature after B-mode batch correction was performed.

T-test was used to determine significant differences between risk groups in relation to the overall abundance of each immune cell type. R package "rstatix" was used for the analysis.

Results

Data Characteristics

TCGA LGG and GBM cohorts were combined by aggregating mRNA-seq readings based on unique patient IDs. This was then split into a training and a test set (Supplementary Figure 2). The data distribution between the training and test sets is comparable after data partitioning was performed on the combined cohorts of TCGA LGG and TCGA GBM. We note that the distribution between clinical variables in the GLASS validation set differs from that of the TCGA cohort (Supplementary Table 2).

Prognostic CHRGs Identified Through Gene Expression and Patient Survival

In total, 50 out of the 133-copper homeostasis-related genes were found to be differentially expressed based on our analysis using 3 different methods (ie, "DESeq2," "edgeR" and "limma-voom"; Supplementary Figure 3A - B). Univariate Cox proportional hazards regression analysis identified 44 DEG associated with the survival of glioma patients with a threshold of $P < .05$. The LASSO regression algorithm was used to calculate regression coefficients which was used to develop the prognostic CHRG signature (Figure 1A-B). A final list of 19 CHRGs were determined to be significantly associated with patient survival and were included in the risk score model (Supplementary Table 3).

Functional Associations of Prognostic CHRG Signature

To assess the function of the 19 prognostic CHRGs, gene set enrichment was performed using Enrichr. 17 out of the 19 prognostic CHRGs were found in 67 GO biological processes, 10 GO molecular functions, and 12 Reactome (2022) pathways (Supplementary Table 4). Figure 1C shows the top enrichments in gene sets and pathways involved in cancer. Genes in the prognostic CHRG signature can be found in processes involved in copper, zinc, and iron responses, lipid formation and remodeling, collagen/fiber formation and organization, vasculature development, immune cell regulation, cell cycle, epithelial to mesenchymal transition and extracellular matrix organization.

To further strengthen the functionality of the CHRG signature, we have analyzed and compared the median mRNA abundance and median dependency scores in 55 glioma cell lines (Figure 1D, Supplementary Table 5). Genes with lower dependency scores have higher essentiality in cell survival or proliferation, such as CDK1, MT1X, and MT1G. Whereas, genes such as ALB, LOXL3, and AQP1 when knocked out result in a slightly more proliferative state in glioma cell lines compared to nonmalignant cell lines.

Validation of Prognostic CHRG Convey Significant Correlation to Survival

To provide additional context for protein-level expression of the prognostic genes, we examined IHC data available through the Human Protein Atlas (Figure 2A, Supplementary Figure 4, and Supplementary Table 1).[28] It is important to note that these IHC data are derived from independent samples and cannot be directly correlated with the mRNA-based risk score model. While this provides valuable biological context, the relationship between mRNA and protein levels is complex and often nonlinear. Future studies will be needed to establish direct correlations between transcript and protein levels in matched samples.

To determine whether the risk score model can be used to predict patient survival, risk scores were calculated based on the expression of the prognostic CHRG signature identified and regression coefficients (Supplementary Table 3) determined through the LASSO regression analysis. Patients in the training and test sets were grouped into high-risk and low-risk groups based on the median risk score determined from the training set (–0.5888). Figure 2B—D shows the distribution of high- and low-risk groups in relation to IDH mutation status and the expression of the prognostic CHRG signature in both the training and test sets.

Patients stratified to the high-risk group significantly correlated to poorer survival compared to the low-risk group ($P < .0001$) in all datasets (Figure 2E—G). The AUC of the ROC curve was analyzed to assess the predictive performance of the prognostic CHRG signature. The AUC of the 1-, 3- and 5-year OS were all above 0.8 in both the training and test sets which shows that the CHRG signature has a strong discriminative ability in predicting survival across these glioma datasets (Figure 2H—J). However, note the moderate discriminative ability of the CHRG signature (AUC = 0.63) in predicting 1-year survival in the independent validation cohort. This could be attributed to the low number of patient IDs with a survival time of 1-year or less. The c-indices calculated were at 0.825 (training set), 0.839 (TCGA test set), and 0.677 (GLASS set). Furthermore, an examination of the Schoenfeld residuals showed that the proportionality assumption of the Cox PH model was satisfied (Supplementary Figure 5).

CHRG Signature-Based Nomogram Model Can Accurately Predict Survival in Glioma Patients

Risk score group, age group, and tumor grade were identified to be significantly associated with survival in a univariate and multivariable Cox regression analysis (Supplementary Table 6). The risk score along with the specified clinical characteristics were used to develop a nomogram model (Figure 3A). The calibration curves show near-accurate survival prediction of the nomogram model based on the CHRG signature risk scores in both

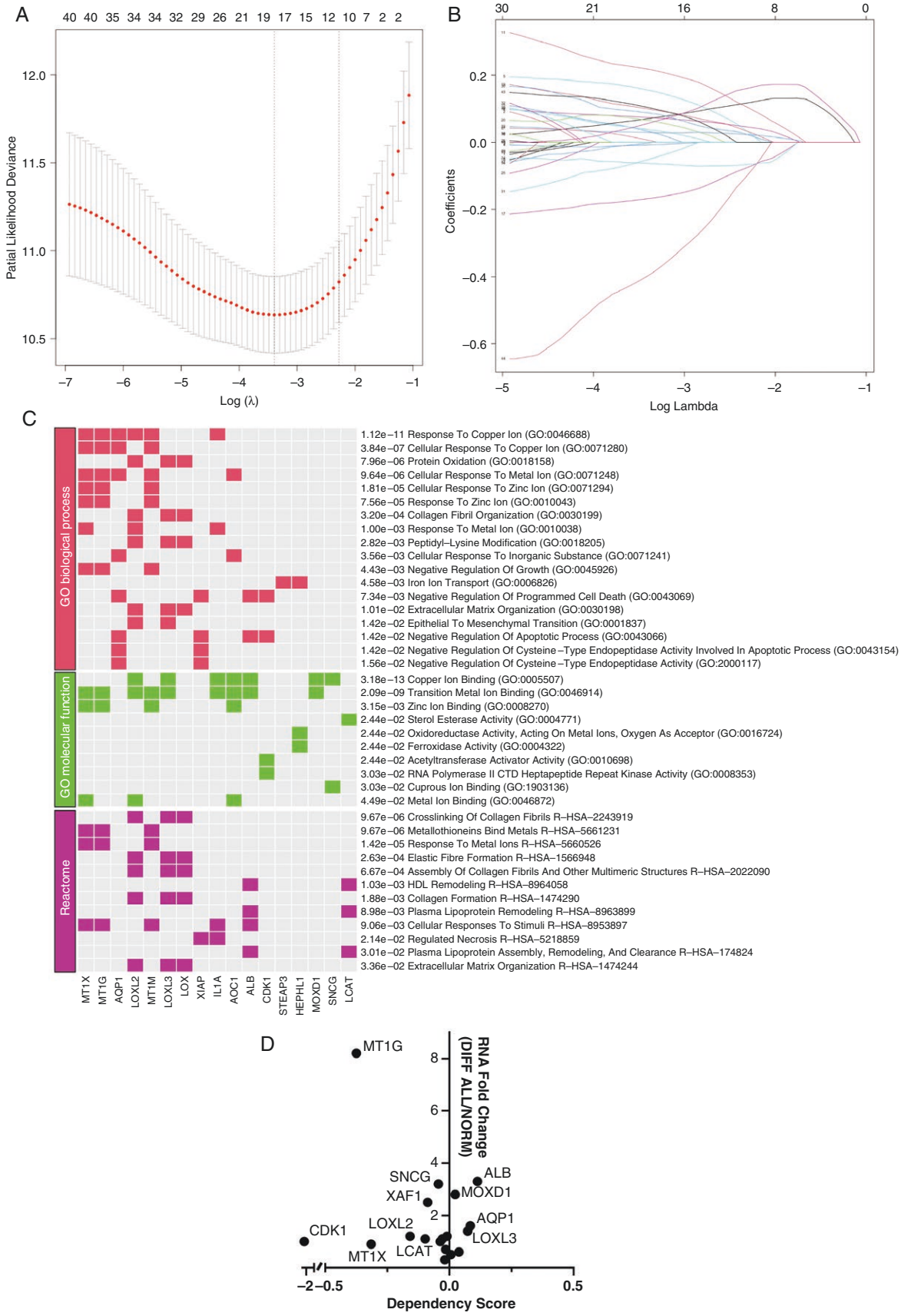

Figure 1. Identification of copper homeostasis-related prognostic genes. (A) 10-fold cross-validation performed to identify robust prognostic genes through the least absolute shrinkage and selection operator (LASSO) regression model. (B) Regression coefficient profiles derived using

the LASSO regression model. (C) Gene set enrichments detected in GO Biological process, GO molecular function and Reactome in order of the adjusted *P*-values. (D) Scatter plot comparing median RNA expression (RNA-sequencing—Expression Public 23Q4) in all diffuse brain cancer cell lines to RNA expression in immortalized neuronal nonmalignant lines, with dependencies (24Q2, Chronos). The data was provided by the Broad Institute Cancer Dependency Map Expression Public 24Q2 (https://depmap.org/portal/).

the training and the test sets (Figure 3B). The AUCs (over 0.8) in both the training and test sets confirm the strong accuracy of this nomogram based on our prognostic CHRG signature in predicting 1-, 3- and 5-year survival in glioma patients. However, like the analysis presented above, the ability of the nomogram model to predict 1-year survival in the GLASS dataset is reduced to moderate accuracy (Figure 3C).

CHRG Signature-Based Nomogram Model Accurately Predicts Survival in Glioma Patients Regardless of IDH Gene Mutation Status

We further determined whether the nomogram model can be applied to patient cohorts grouped based on adult-type diffuse glioma WHO CNS5 classification. Both the TCGA and GLASS sample datasets were stratified between glioblastoma, IDH-wild type, astrocytoma, IDH-mutant or oligodendroglioma, IDH-mutant, 1p/19q codeleted (Figure 4). For brevity, these tumor groups will be addressed as glioblastoma, astrocytoma, and oligodendroglioma from this point forward. This was performed to establish if the nomogram model can be used to account for the most recent change in the WHO classification of CNS tumors where molecular characteristics such as IDH mutation and 1p/19q codeletion are used to classify and differentiate high-grade glioblastoma, and lower-grade oligodendroglioma and astrocytomas.[1]

An inverse pattern of mRNA expression was observed between high-risk and low-risk groups within and across each WHO CNS5 classification (Figure 4A). Genes such as *ALB, LCAT, MT-CO2, SNCG, MT1X,* and *XIAP* are highly expressed in both astrocytoma and oligodendroglioma. Conversely, *CDK1, LOX, LOXL2, LOXL3, XAF1, AOC1, AQP1, MOXD1*, and *STEAP3* show high expression in glioblastoma. High expression of *MT1G* and *MT1M* was observed in oligodendroglioma and glioblastoma, while *HEPHL1* and *IL1A* were highly expressed in astrocytoma and glioblastoma (Supplementary Figure 6). As observed in the training and test sets, risk score grouping shows that high-risk groups had poorer survival than low-risk groups ($P < .05$) in the different tumor classification groups (Figure 4B–D). The AUC of the ROC curve was further evaluated within each tumor classification group. The AUCs depict a moderate to strong predictive ability of the nomogram model within the tumor classification groups (Figure 4E–G).

Clinical, Histological, and Molecular Landscape of Patients Within Risk Groups

To understand the distribution of clinical characteristics within each risk group, a stratified analysis was performed (Supplementary Figure 7). Amongst all clinical characteristics, gender is almost equally distributed within risk groups. More patients over the age of 39 years were observed in the high-risk group while age groups were equally distributed in the low-risk group. Patients diagnosed with glioblastoma are majorly observed within the high-risk group. IDH-mutant astrocytoma and oligodendrogliomas were more frequently observed in the low-risk group with some proportions found in the high-risk group. Methylated and unmethylated MGMT is almost evenly distributed in the high-risk group with more methylated MGMT samples observed in the low-risk group.

Risk Score Grouping Confers With Expected Immune Cell Estimates and mRNA Expression of Immune Checkpoints in Glioma

To investigate whether the CHRG signature can be used to predict patient stratification into immune-related therapies, risk score grouping was analyzed to determine correlations with immune cell estimates and expression of immune cell markers. Intracellular copper levels have been shown to modulate immune checkpoint expression such as PD-L1.[6] This coincides with the enrichment observed in the CHRG signature. Based on this we further investigated the correlation of risk scores to immune cell populations observed within these patient samples. Firstly, the absolute immune cell proportions were estimated using the CIBERSORT deconvolution algorithm.[31,32] Following this, a correlation matrix was performed where it was observed that patient risk scores have an overall moderately positive correlation with the expression of macrophage M0 (0.57, $P < .001$), M1 (0.45, $P < .001$) and M2 (0.55, $P < .001$) signatures (Figure 5A—C). Further examination of the association between risk score grouping and these immune cell populations shows a statistically significant difference between low- and high-risk groups (Figure 5D). This is in line with current literature indicating that glioma-associated macrophages are linked to poorer survival due to their intrinsic properties that promote tumor growth.[33]

Moreover, the expression of all immune checkpoints was significantly higher in the high-risk group than in the low-risk group (Figure 6A). Further investigation shows moderate to strong correlations between the cluster of differentiation 274 (*CD274* a.k.a. *PD-L1*), Programmed cell death protein 1 (*PDCD1* a.k.a. *PD1*), Hepatitis A Virus Cellular Receptor 2 (*HAVCR2* a.k.a. *TIM3*), Inducible T-Cell Costimulator (*ICOS*), Inducible T-Cell Costimulator Ligand (*ICOSLG*), and GATA Binding Protein 3 (*GATA3*), and various genes within the CHRG signature (Figure 6B—D). This again coincides with existing evidence that higher expression of the aforementioned immune checkpoints is linked to poorer survival. This indicates the potential use of this risk score model as a determinant for immune-targeted therapies.

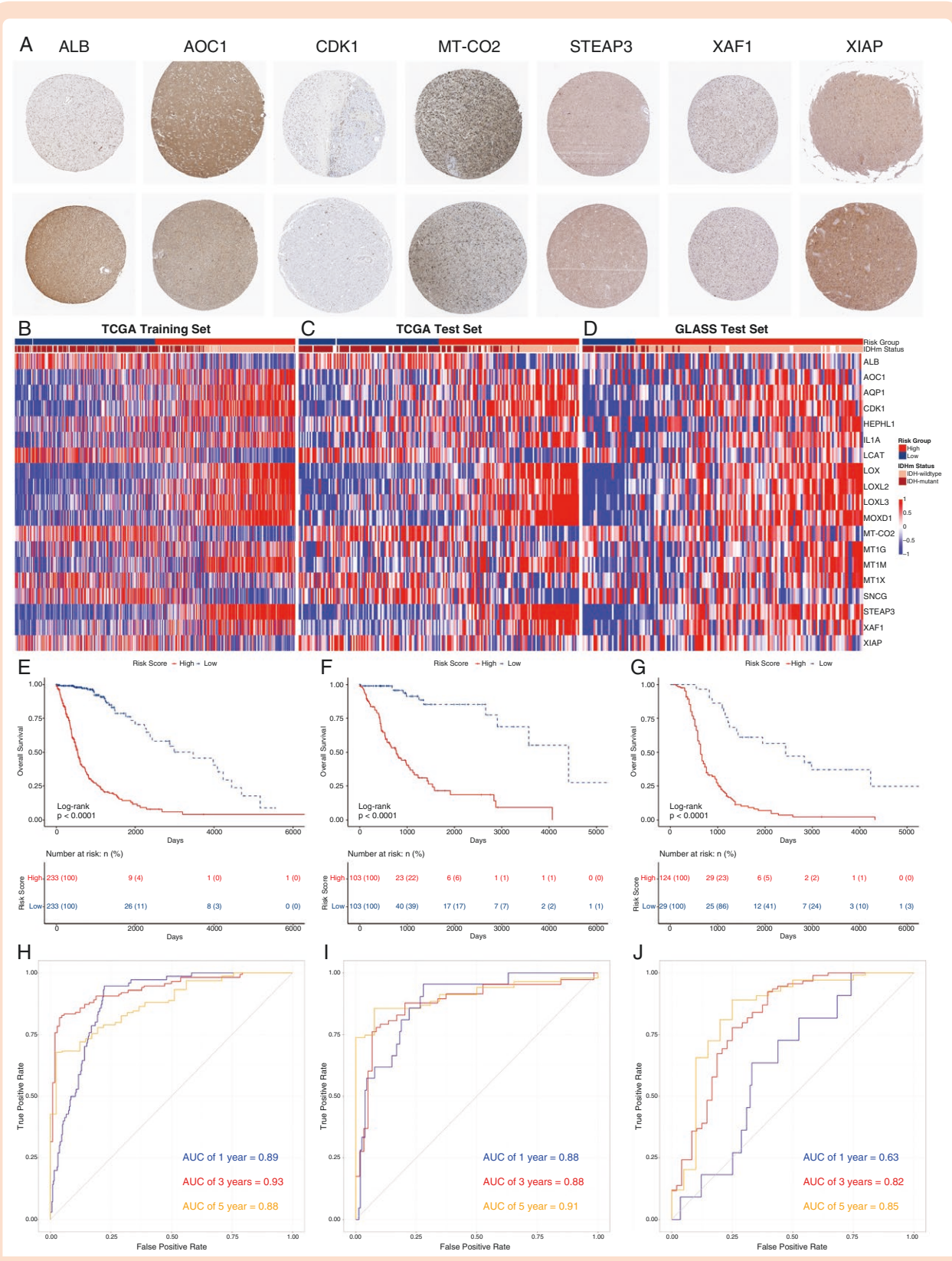

Figure 2. Identification of copper metabolism-related prognostic signature for OS of high- and lower-grade glioma. (A) Representative IHC images from the Human Protein Atlas showing protein expression patterns of key genes from the signature in glioma tissues. These images are from an independent dataset and serve to illustrate protein presence in glioma tissue, but do not directly correspond to the mRNA-based risk stratification model. Image credit: Human Protein Atlas (www.proteinatlas.org).[28] Images available at the following URL: v23.proteinatlas.org/humancell. Risk score modeling performed on training set and test sets derived from the TCGA glioma (B, E, H) training and (C, F, I) test. Validation of the risk score model using an independent cohort from the (D, G, J) GLASS consortium. (B—D) Gene expression distribution across risk score groups

annotated with overall survival and IDH1 mutation status. (E–G) Kaplan–meier plots showing significant survival difference between high and low risk groups. (H–J) ROC curves showing the diagnostic ability of predicting survival in a glioma cohort using the identified prognostic copper-homeostasis-related gene.

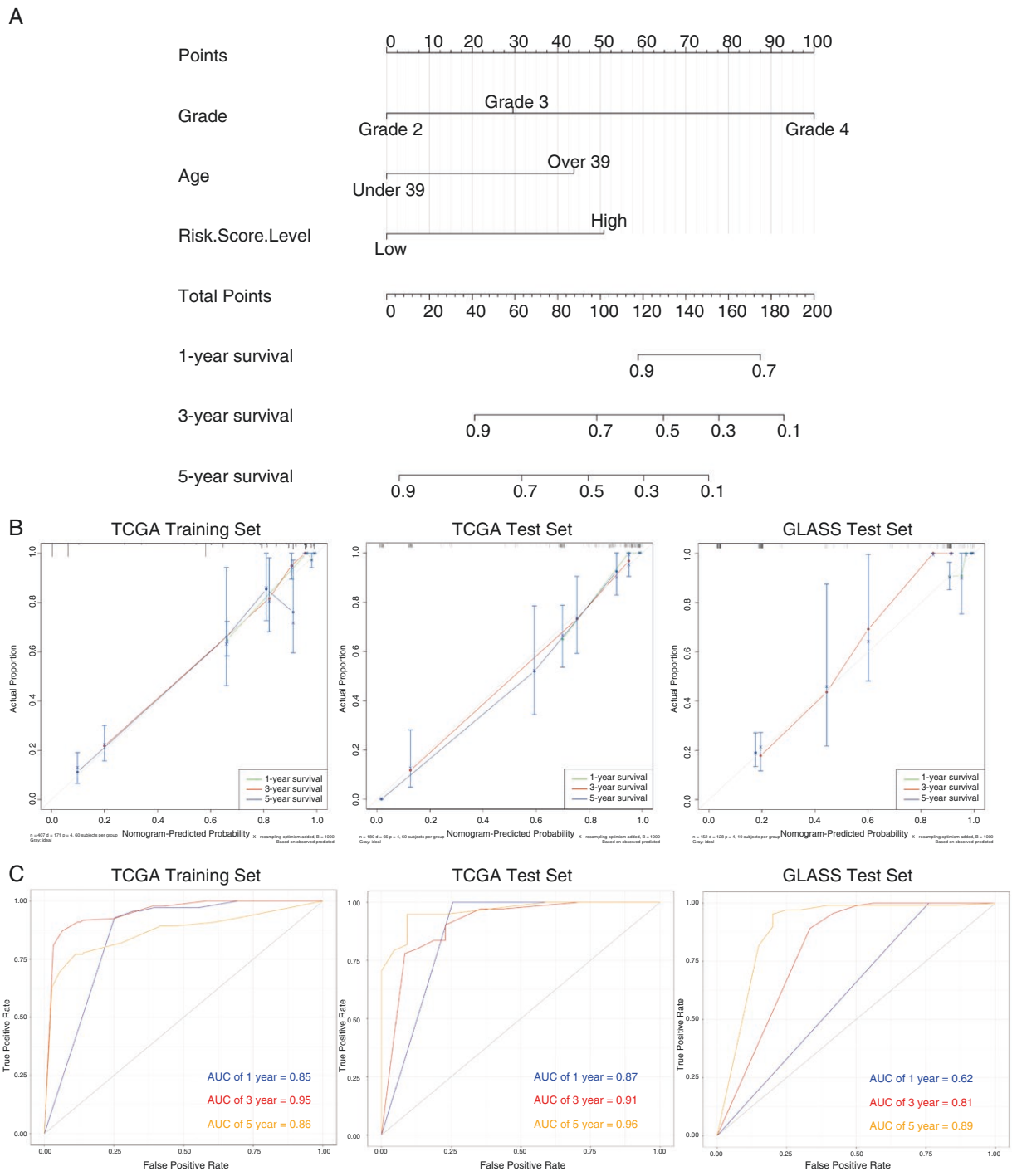

Figure 3. Construction and validation of a prognostic nomogram model using risk score stratification based on copper metabolism related genes. (A) Nomogram model constructed to determine probability of survival in 1, 3 and 5 years for adult-type diffuse glioma patients. (B) Calibration curves of the nomogram model to determine the validity of the model in predicting survival in both the training and test sets. The plot shows nomogram-predicted probability of survival (*x*-axis) against the actual overall survival (y-axis) observed for 1, 3 and 5 years. (C) ROC curves to validate the prognostic ability of the nomogram model to determine probability of 1-, 3- and 5-year overall survival in glioma patients.

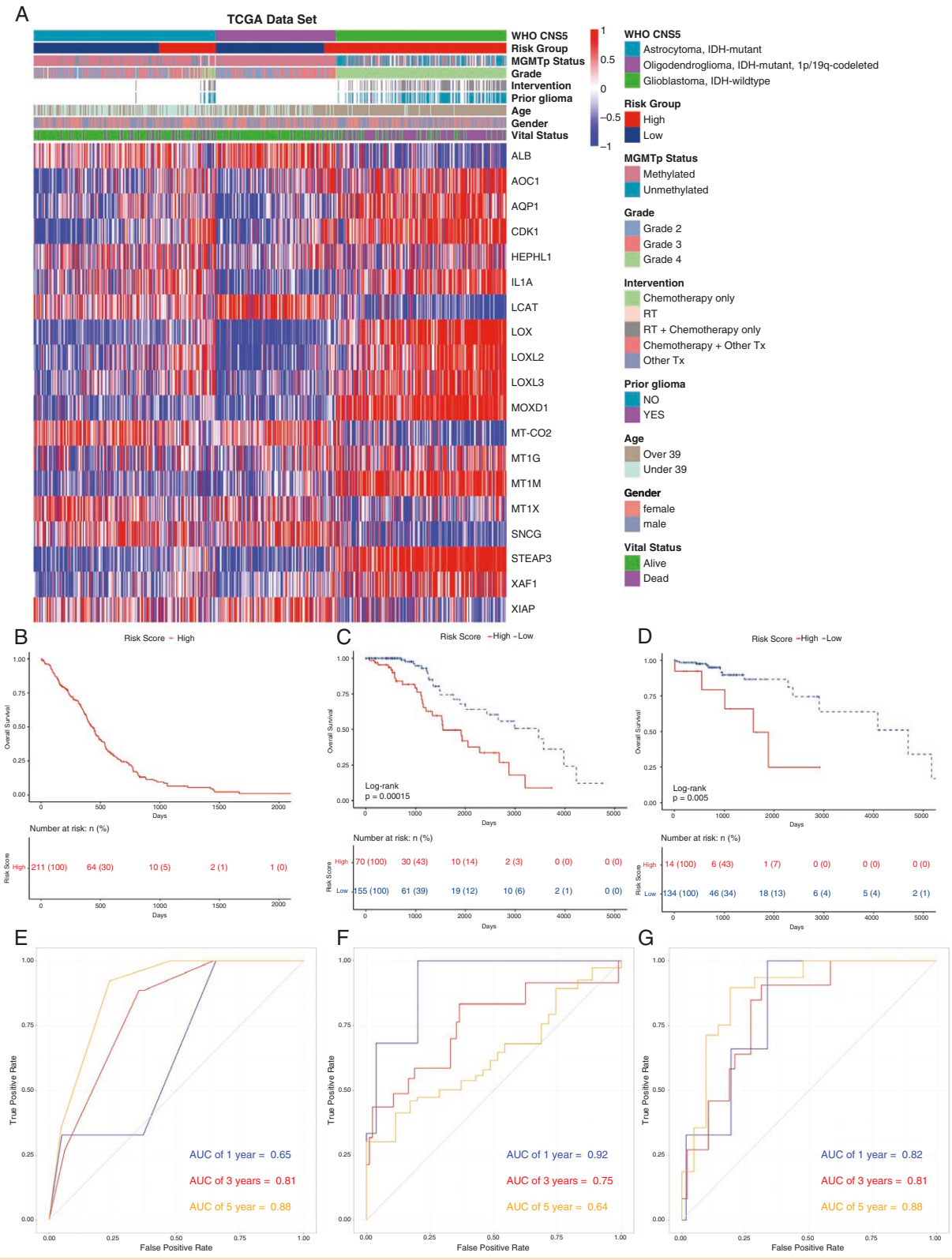

Figure 4. Patient survival classified based on WHO CNS5 tumor classification correlate to prognostic risk model. (A) Gene expression distribution across clinical annotations and risk groups. (B—D) Kaplan–meier plots showing significant survival difference between high and low risk groups in glioblastoma, IDH-wild type (B), astrocytoma, IDH-mutant (C), and oligodendroglioma, IDH-mutant, 1p/19q codeleted (D) tumors. ROC curves showing the diagnostic ability of predicting survival in glioblastoma, IDH-wild type (E), astrocytoma, IDH-mutant (F), and oligodendroglioma, IDH-mutant, 1p/19q codeleted (G) tumors.

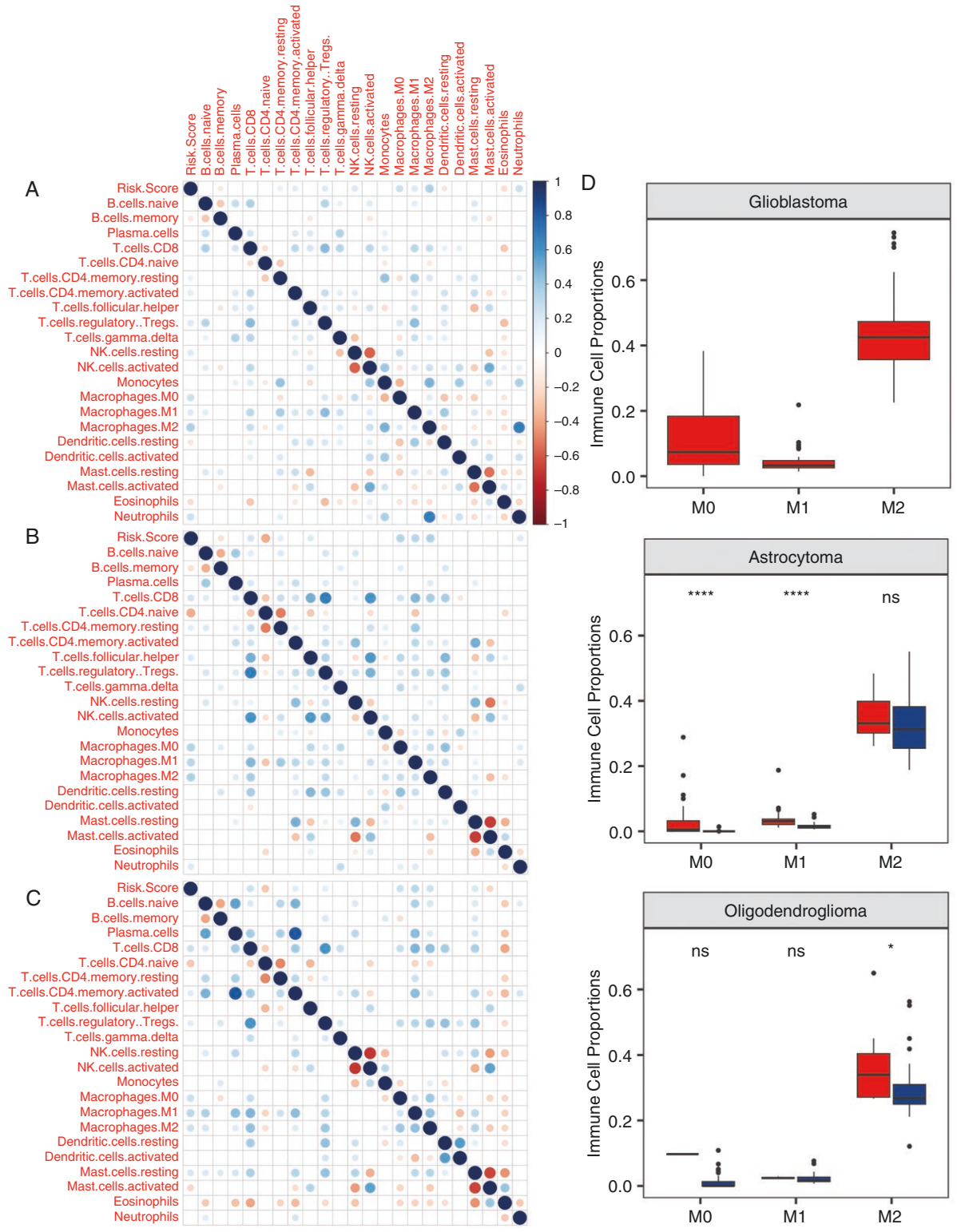

Figure 5. Risk score and signature correlations with immune cell proportions. Correlation matrix between 22 immune cell types and patient risk scores in (A) GBM, IDH-wild type, (B) Astrocytoma, IDH-mutant, (C) Oligodendroglioma, IDH-mutant, 1p/19q codeleted. (D) Boxplots showing differences in immune cell proportions of macrophage phenotypes between high and low-risk groups. Legends: (A—C) Size of circles correspond to R coefficient values. Blank boxes do not satisfy statistical significance ($P < .05$). (D) High-risk group are represented by the red (first) boxplot. Low risk group are represented by the blue (second) boxplot.

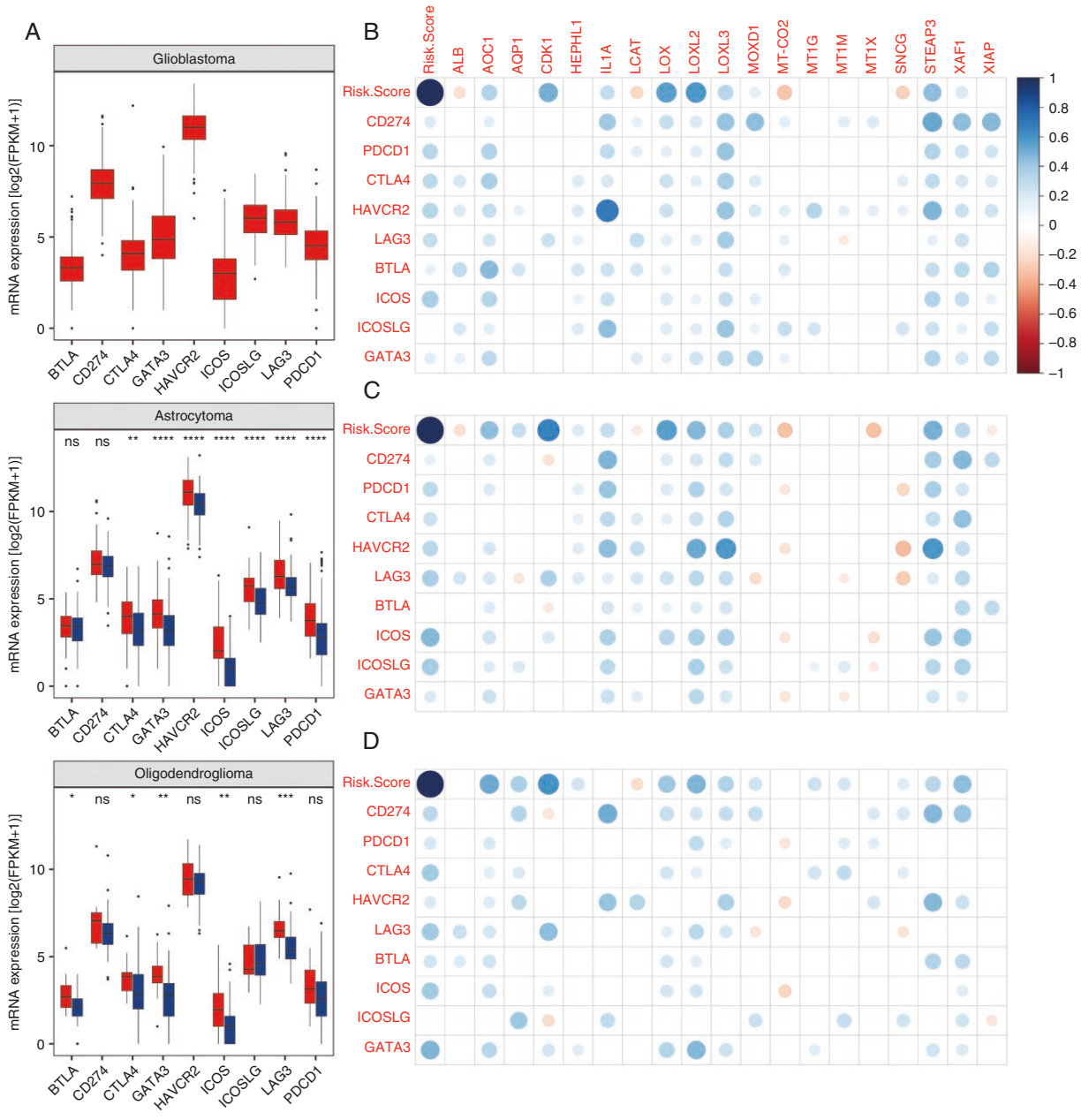

Figure 6. Risk score and signature correlations with immune checkpoint mRNA expressions. (A) mRNA expression [log2(FPKM + 1)] of different immune checkpoints in glioma samples stratified between high- and low-risk groups. Matrices showing correlations between risk score, immune checkpoints (y-axis) and CHRG signature (*x*-axis) in (B) GBM, IDH-wild type, (C) Astrocytoma, IDH-mutant, (D) Oligodendroglioma, IDH-mutant, 1p/19q codeleted. Legends: (A—C) Size of circles correspond to R coefficient values. Blank boxes do not satisfy statistical significance ($P < .05$). (D) High-risk group are represented by the red (first) boxplot. Low risk group are represented by the blue (second) boxplot.

Discussion

Gliomas are a heterogeneous and highly invasive group of tumors originating from glial cells in the brain. Gliomas occurring in adults (mean age 41 years old) are currently classified as astrocytoma IDH-mutant, oligodendroglioma IDH-mutant and 1p/19q codeleted, and glioblastoma IDH wild-type.[1,34] Survival between tumor subtypes can widely vary from having a 14-month median survival in GBM to an average survival of 7 years in lower-grade gliomas (LrGG; ie, Grade 2/3 astrocytomas and oligodendrogliomas). Despite survival times being longer in LrGGs, most if not all will progress into a high-grade glioma with a much worse prognosis.

Imbalances in copper levels have been linked to the pathogenesis and progression of diverse diseases, including cancer. This association is supported by research

revealing notably elevated copper concentrations in cancerous tissues, including gliomas, in contrast to healthy cellular environments.[4] Efforts to regulate copper levels, particularly in glioblastoma, have been explored; however, these endeavors have not yielded enhanced patient survival rates.[35,36] This lack of positive outcomes might be attributed to the absence of patient stratification for tailored treatments, resulting in a uniform therapeutic approach that overlooks individual variabilities.

While our team leads clinical trials evaluating copper chelation in breast cancer (NCT00195091), lung cancer, and neuroblastoma, this study focuses on establishing a prognostic gene signature for glioma patient stratification based on survival outcomes. Although these findings may inform future studies of copper modulation treatments, the predictive value of this signature for treatment response would require additional preclinical and clinical validation.

A review of the literature identified 12 studies developing copper-related gene signatures for glioma risk models.[10,13–22,37] This study advances the field through key innovations: (1) an unbiased approach incorporating 133 copper-related genes from MSigDB, (2) WHO-CNS5 reannotation of TCGA data to correct tumor classification and grading, and (3) integration of 3 differential expression analysis methods. These methodological refinements yielded improved predictive performance, demonstrated by superior ROC curve analysis, establishing a more reliable prognostic framework for glioma patients.

This study has developed a predictive model utilizing a 19-CHRG risk signature along with age, tumor grade, and IDH mutation status to accurately predict survival. Genes in the CHRG signature are mostly involved in processes in copper, zinc, and iron responses, lipid formation and remodeling, collagen/fiber formation and organization, vasculature development, immune cell regulation, cell cycle, epithelial to mesenchymal transition and extracellular matrix organization. Of the 19 CHRGs in the risk signature, the following are highly enriched and are notable in their link to copper within various biological processes in the body. *LOX, LOXL2, and LOXL3* are copper-dependent amine oxidases that promote crosslinking of elastin and collagen within the extracellular matrix. *MTIG*, *MTIM*, and *MT1X* are metallothionines directly involved in intracellular copper binding.[38] *XIAP* is a caspase inhibitor that directly binds intracellular copper.[39] *LCAT* and *ALB*, both involved in HDL remodeling, rely on copper, with LCAT's enzymatic activity being copper-dependent and ALB binding copper in the bloodstream.[40,41] CDK1/cyclin B kinase is significantly inhibited by oxindolimine-copper(II) complexes, with copper enhancing activity by providing stronger interactions with the ATP-binding site and inducing a more rigid conformation compared to the free ligand.[42] *AOC1* encodes for a copper-containing enzyme that deaminates putrescine, high levels of this enzyme are seen in highly malignant cancerous processes.[43,44] *AQP1* encodes for a widely expressed water channel regulated by copper.[5,45] *IL1A* is a pro-angiogenic peptide and pro-inflammatory cytokine that gets released in a copper-dependent manner.[46,47] *STEAP3* is a cupric reductase that promotes cancer cell proliferation through increased intracellular uptake.[48] *MOXD1* is a copper-dependent monooxygenase that is highly expressed and found to promote cell viability, proliferation, migration, invasion, and tumorigenesis of GBM cells.[49] *XAF1* is a tumor suppressor gene that antagonizes MT2A protein expression, a known copper-binding protein.[50] Therefore, high *XAF1* expression may be correlated to increased free intracellular copper due to the deactivation of MT2A.

The risk score model identifies patients over the age of 39 as high-risk in line with literature that shows older patients have higher levels of copper.[51,52] Majority of the samples with glioblastoma were stratified as high-risk which again corroborates existing literature showing that higher copper levels are observed in more malignant brain tumors.[4]

To understand the clinical validity of our predictive model, we analyzed correlations between the CHRG signature and mRNA expression of various immune phenotypes and immune checkpoints from the same patient cohort. Risk scores showed a significant positive correlation to different macrophage subtypes and a negative correlation to naïve CD4 T-cell which confers to already published literature. It is worth noting that our predictive model, based on CHRG expression, stratifies patients with dysregulated immune checkpoints (ie, *CD274* (*PD-L1*), *PDCD1* (*PD-1*), *HAVCR2* (*TIM3*), *ICOS*, *ICOSLG*, and *GATA3*). This is in line with recent literature where a high correlation was observed between the expression of some checkpoints, such as PD-L1, and intratumoral copper levels.[6] This strengthens the use of our CHRG signature as a biomarker to predict which patients have the likelihood to respond to immunotherapies.

This study paves the way for future investigations on the interplay of copper-related genes in adult gliomas. This will in turn allow for a better understanding of the relationship between copper homeostasis and the immune system which could underpin novel combination therapies with copper-targeting drugs and immunotherapies in the future. It also suggests exploring similar aspects of pediatric low- and high-grade gliomas and correlate with their molecular subsets, which could potentially establish novel approaches to risk stratification, biomarkers of disease or treatment response, and personalized therapies.

Supplementary Material

Supplementary material is available online at *Neuro-Oncology Advances* (https://academic.oup.com/noa).

Keywords

copper | cuproplasia | glioma | immunotherapy | personalized medicine

Lay Summary

Diffuse gliomas are a common type of brain tumor that is hard to treat. Some patients live for a short time, while others survive longer. The authors of this study wanted to find out whether the

body's ability to manage copper, an important mineral that has been found to influence cancer growth, affected how long patients with gliomas lived. To do this, they looked at genetic data from patients with these tumors. Their results showed that 19 copper-related genes were linked to tumor growth and survival, with higher levels of these genes linked to shorter survival times.

Funding

Higher Thinking Brain Cancer Research Fund (Munificent Foundation).

Acknowledgments

We would like to express our deepest gratitude to the Munificent Foundation for their generous support through the Higher Thinking Brain Cancer Research Fund, which made this research possible.

Conflict of interest

The authors declare no conflict of interests.

Authorship statement

Contribution or task: All authors approved this submission. Project conceptualization—T.R.J. Statistical analyses—T.R.J. and J.D. Data analysis—T.R.J., J.D., V.P. and J.B. Critical review and manuscript editing for important intellectual content—T.R.J., J.D., V.P., O.V., R.C., T.S.H., E.S.K., and S.N.

Data availability

Data sharing is not applicable to this article as no new datasets were generated during the current study. All datasets used for analysis in this study are freely and publicly available at UCSC Xena: https://doi.org/10.1038/s41587-020-0546-8[23] and Synapse: https://www.synapse.org/glass.24 No new data have been generated in this study. Codes used for reannotation and analysis are available at https://github.com/tonijue/CHRGsignature_RiskModel.git

Declaration of generative AI and AI-assisted technologies in the writing process

During the preparation of this manuscript the authors used ChatGPT to improve the readability and language of the manuscript. After using this tool, the authors reviewed and heavily revised the content as needed and take full responsibility for the content of this publication.

Affiliations

Children's Cancer Institute, Lowy Cancer Research Centre, UNSW Sydney, Randwick, New South Wales, Australia 1466 (T.R.J., J.L.B., T.S.H., R.C.); Ingham Institute for Applied Medical Research, Liverpool, New South Wales, Australia 2170 (J.D.); South Western Sydney Clinical School, University of New South Wales, Liverpool, New South Wales, Australia 2170 (J.D., E.S.K.); School of Biomedical Sciences, Faculty of Medicine and Health, University of New South Wales, Sydney, New South Wales, Australia 1466 (V.V.H.P., O.V.); School of Clinical Medicine, University of New South Wales, Sydney, New South Wales, Australia 1466 (T.R.J., J.L.B., T.S.H., R.C.); Kids Cancer Centre, Sydney Children's Hospital, Randwick, New South Wales, Australia 2031 (S.N.); Department of Radiation Oncology, Liverpool Cancer Therapy Centre, Liverpool, New South Wales, Australia 2170 (E.S.K.)

References

1. Louis DN, Perry A, Wesseling P, et al. The 2021 WHO Classification of Tumors of the Central Nervous System: A summary. *Neuro Oncol.* 2021;23(8):1231–1251.
2. Ostrom QT, Price M, Neff C, et al. CBTRUS Statistical Report: Primary brain and other central nervous system tumors diagnosed in the United States in 2015–2019. *Neuro Oncol.* 2022;24(suppl_5):v1–v95.
3. Panichelli P, Villano C, Cistaro A, et al. Imaging of brain tumors with Copper-64 chloride: Early experience and results. *Cancer Biother Radiopharm.* 2016;31(5):159–167.
4. Yoshida D, Ikeda Y, Nakazawa S. Quantitative analysis of copper, zinc and copper/zinc ratio in selected human brain tumors. *J Neurooncol.* 1993;16(2):109–115.
5. Ge EJ, Bush AI, Casini A, et al. Connecting copper and cancer: From transition metal signalling to metalloplasia. *Nat Rev Cancer.* 2022;22(2):102–113.
6. Voli F, Valli E, Lerra L, et al. Intratumoral copper modulates PD-L1 expression and influences tumor immune evasion. *Cancer Res.* 2020;80(19):4129–4144.
7. Hanahan D, Weinberg RA. Hallmarks of cancer: The next generation. *Cell.* 2011;144(5):646–674.
8. Zhao S, Zhang X, Gao F, et al. Identification of copper metabolism-related subtypes and establishment of the prognostic model in ovarian cancer. Original Research. *Front Endocrinol.* 2023;14:1145797.
9. Lin J, Luo B, Yu X, et al. Copper metabolism patterns and tumor microenvironment characterization in colon adenocarcinoma. *Front Oncol.* 2022;12:959273.
10. Li L, Leng W, Chen J, et al. Identification of a copper metabolism-related gene signature for predicting prognosis and immune response in glioma. *Cancer Med.* 2023;12(8):10123–10137.
11. Sun D, Zhang H, Zhang C. Development of a novel copper metabolism-related risk model to predict prognosis and tumor microenvironment

of patients with stomach adenocarcinoma. Original Research. *Front Pharmacol.* 2023;14:1185418.
12. Chang W, Li H, Zhong L, et al. Development of a copper metabolism-related gene signature in lung adenocarcinoma. Original Research. *Front Immunol.* 2022;13:1040668.
13. Bao JH, Lu WC, Duan H, et al. Identification of a novel cuproptosis-related gene signature and integrative analyses in patients with lower-grade gliomas. *Front Immunol.* 2022;13:933973.
14. Feng S, Zhang Y, Zhu H, et al. Cuproptosis facilitates immune activation but promotes immune escape, and a machine learning-based cuproptosis-related signature is identified for predicting prognosis and immunotherapy response of gliomas. *CNS Neurosci Ther.* 2024;30(2):e14380.
15. Chen B, Zhou X, Yang L, et al. A cuproptosis activation scoring model predicts neoplasm-immunity interactions and personalized treatments in glioma. *Comput Biol Med.* 2022;148:105924.
16. Zhang Z, Wang B, Xu X, Xin T. Cuproptosis-related gene signature stratifies lower-grade glioma patients and predicts immune characteristics. *Front Genet.* 2022;13:1036460.
17. Zhang M, Liu X, Wang D, et al. A novel cuproptosis-related gene signature to predict prognosis in Glioma. *BMC Cancer.* 2023;23(1):237.
18. Wu Z, Li W, Zhu H, et al. Identification of cuproptosis-related subtypes and the development of a prognostic model in glioma. *Front Genet.* 2023;14:1124439.
19. Shen N, Chen S, Liu D, Min X, Tan Q. Cuproptosis-related classification and personalized treatment in lower-grade gliomas to prompt precise oncology. *J Gene Med.* 2023;25(6):e3486.
20. Chen S, Zhang S, Yuan Y, et al. Prognostic value of cuproptosis-related genes signature and its impact on the reshaped immune microenvironment of glioma. *Front Pharmacol.* 2022;13:1016520.
21. Chen P, Han H, Wang X, Wang B, Wang Z. Novel cuproptosis-related gene signature for precise identification of high-risk populations in low-grade gliomas. *Mediators Inflamm.* 2023;2023:6232620.
22. Wang W, Lu Z, Wang M, et al. The cuproptosis-related signature associated with the tumor environment and prognosis of patients with glioma. *Front Immunol.* 2022;13:998236.
23. Goldman MJ, Craft B, Hastie M, et al. Visualizing and interpreting cancer genomics data via the Xena platform. *Nat Biotechnol.* 2020;38(6):675–678.
24. Barthel FP, Johnson KC, Varn FS, et al; GLASS Consortium. Longitudinal molecular trajectories of diffuse glioma in adults. *Nature.* 2019;576(7785):112–120.
25. Zakharova G, Efimov V, Raevskiy M, et al. Reclassification of TCGA diffuse glioma profiles linked to transcriptomic, epigenetic, genomic and clinical data, according to the 2021 WHO CNS Tumor Classification. *Int J Mol Sci.* 2022;24(1):157.
26. Friedman J, Hastie T, Tibshirani R. Regularization paths for generalized linear models via coordinate descent. *J Stat Softw.* 2010;33(1):1–22.
27. Blanche P, Dartigues JF, Jacqmin-Gadda H. Estimating and comparing time-dependent areas under receiver operating characteristic curves for censored event times with competing risks. *Stat Med.* 2013;32(30):5381–5397.
28. Uhlén M, Björling E, Agaton C, et al. A human protein atlas for normal and cancer tissues based on antibody proteomics. *Mol Cell Proteomics : MCP.* 2005;4(12):1920–1932.
29. Kuleshov MV, Jones MR, Rouillard AD, et al. Enrichr: A comprehensive gene set enrichment analysis web server 2016 update. *Nucleic Acids Res.* 2016;44(W1):W90–W97.
30. Tsherniak A, Vazquez F, Montgomery PG, et al. Defining a cancer dependency map. *Cell.* 2017;170(3):564–576.e16.
31. Chen B, Khodadoust MS, Liu CL, Newman AM, Alizadeh AA. Profiling tumor infiltrating immune cells with CIBERSORT. *Methods Mol Biol.* 2018;1711:243–259.
32. Newman AM, Liu CL, Green MR, et al. Robust enumeration of cell subsets from tissue expression profiles. *Nat Methods.* 2015;12(5):453–457.
33. Wei J, Chen P, Gupta P, et al. Immune biology of glioma-associated macrophages and microglia: Functional and therapeutic implications. *Neuro Oncol.* 2019;22(2):180–194.
34. Claus EB, Walsh KM, Wiencke JK, et al. Survival and low-grade glioma: The emergence of genetic information. *Neurosurg Focus.* 2015;38(1):E6.
35. Brem S, Grossman SA, Carson KA, et al; New Approaches to Brain Tumor Therapy CNS Consortium. Phase 2 trial of copper depletion and penicillamine as antiangiogenesis therapy of glioblastoma. *Neuro Oncol.* 2005;7(3):246–253.
36. Werlenius K, Kinhult S, Solheim TS, et al. Effect of disulfiram and copper plus chemotherapy vs chemotherapy alone on survival in patients with recurrent glioblastoma: A randomized clinical trial. *JAMA Netw Open.* 2023;6(3):e234149–e234149.
37. Zeng H-L, Li H, Yang Q, Li C-X. Transcriptomic characterization of copper-binding proteins for predicting prognosis in glioma. *Brain Sci.* 2023;13(10):1460.
38. Si M, Lang J. The roles of metallothioneins in carcinogenesis. *J Hematol Oncol.* 2018;11(1):107.
39. Hou M-M, Polykretis P, Luchinat E, et al. Solution structure and interaction with copper in vitro and in living cells of the first BIR domain of XIAP. *Sci Rep.* 2017;7(1):16630.
40. Song X, Wang W, Li Z, Zhang D. Association between serum copper and serum lipids in adults. *Ann Nutr Metab.* 2018;73(4):282–289.
41. Vazquez-Moreno M, Sandoval-Castillo M, Rios-Lugo MJ, et al. Overweight and obesity are positively associated with serum copper levels in Mexican schoolchildren. *Biol Trace Elem Res.* 2023;201(6):2744–2749.
42. Miguel RB, Petersen PA, Gonzales-Zubiate FA, et al. Inhibition of cyclin-dependent kinase CDK1 by oxindolimine ligands and corresponding copper and zinc complexes. *J Biol Inorg Chem.* 2015;20(7):1205–1217.
43. Chanda R, Ganguly AK. Diamine-oxidase activity and tissue di- and polyamine contents of human ovarian, cervical and endometrial carcinoma. *Cancer Lett.* 1995;89(1):23–28.
44. Elmore BO, Bollinger JA, Dooley DM. Human kidney diamine oxidase: Heterologous expression, purification, and characterization. *J Biol Inorg Chem.* 2002;7(6):565–579.
45. Wittekindt OH, Dietl P. Aquaporins in the lung. *Pflugers Archiv : Eur j Physiol.* 2019;471(4):519–532.
46. Prudovsky I, Mandinova A, Soldi R, et al. The non-classical export routes: FGF1 and IL-1α point the way. *J Cell Sci.* 2003;116(24):4871–4881.
47. Mandinova A, Soldi R, Graziani I, et al. S100A13 mediates the copper-dependent stress-induced release of IL-1alpha from both human U937 and murine NIH 3T3 cells. *J Cell Sci.* 2003;116(Pt 13):2687–2696.
48. Knutson MD. Steap proteins: Implications for iron and copper metabolism. *Nutr Rev.* 2007;65(7):335–340.
49. Shi P, Xu J, Xia F, et al. MOXD1 knockdown suppresses the proliferation and tumor growth of glioblastoma cells via ER stress-inducing apoptosis. *Cell Death Discovery.* 2022;8(1):174.
50. Shin C-H, Lee M-G, Han J, et al. Identification of XAF1–MT2A mutual antagonism as a molecular switch in cell-fate decisions under stressful conditions. *Proc Natl Acad Sci USA.* 2017;114(22):5683–5688.
51. Gonzalez-Alcocer A, Gopar-Cuevas Y, Soto-Dominguez A, et al. Combined chronic copper exposure and aging lead to neurotoxicity in vivo. *Neurotoxicology.* 2023;95:181–192.
52. Peng F, Xie F, Muzik O. Alteration of copper fluxes in brain aging: A longitudinal study in rodent using (64)CuCl(2)-PET/CT. *Aging Dis.* 2018;9(1):109–118.